

An addendum on iterated torus knots

William W. Menasco *

University at Buffalo

Buffalo, New York 14260

June 14, 2021

1 Introduction

In Theorem 1.2 of the paper [M1] the author claimed to have proved that all transversal knots whose topological knot type is that of an iterated torus knot (we call them *cable knots*) are transversally simple. That theorem is false, and the Erratum [M2] identifies the gap. The purpose of this paper is to explore the situation more deeply, in order to pinpoint exactly which cable knots are *not* transversally simple. The class is subtle and interesting. We will recover the strength of the main theorem in [M1], in the sense that we will be able to prove a strong theorem about cable knots, but the theorem itself is more subtle than Theorem 1.2 of [M1].

Before we can state the main results in this paper we need to set up some machinery. The reader should recall that a closed braid X is *exchange reducible* to a closed braid Y if through a sequence of exchange moves, destabilizations and braid isotopies we can take X to Y . In the case of cable knots saying that a specified class is *exchange reducible* means that it is exchange reducible to the standard braid representation of minimal index. See Figure 1. Recall also that in [BW] it was established that exchange reducible closed braids representing oriented knots are transversally simple when the braids are viewed as transversal knots in the standard contact structure of \mathbb{R}^3 or S^3 . The key question for us is to understand which cable knots are exchange-reducible and

*partially supported by NSF grant #DMS 0306062

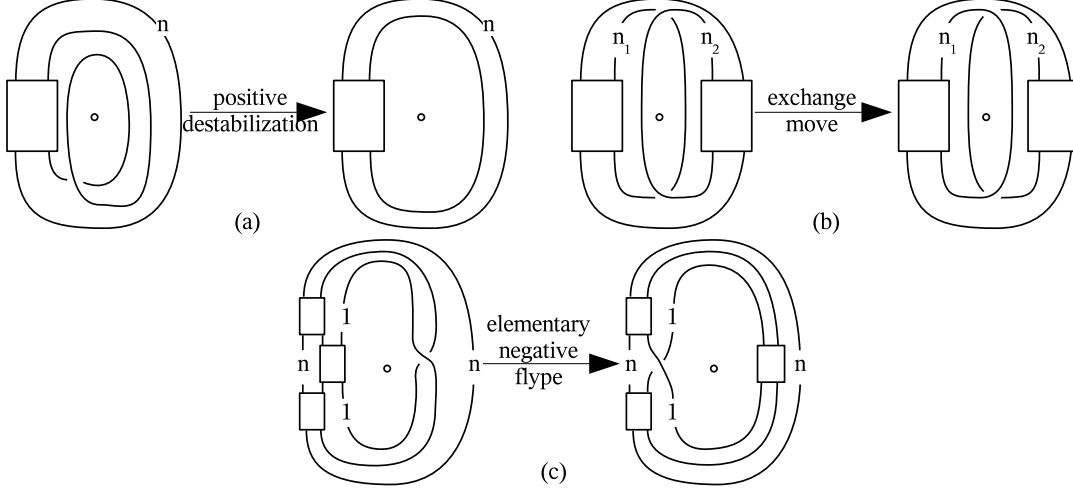


Figure 1: The illustration indicates that some of the strands in the block-strand diagrams can be weight, i.e. multiple parallel strands.

which ones are not. To specify the large subclass of cable knots that are not exchange reducible we need to develop a new mode of representing knots. It is first useful to set up a coordinate system for $(\mathbb{R}^3, \{z\text{-axis}\}) \subset (S^3, \mathbf{A})$. Let (ρ, θ, z) be the classical cylindrical coordinate system for \mathbb{R}^3 . We specify notation for the unit cylinder, $\mathcal{T}_1 = \{(\rho, \theta, z) | \rho = 1\}$; and level planes, $P_{z_0} = \{(\rho, \theta, z) | z = z_0 (= \{\text{constant}\})\}$.

As in [M1] $\mathbf{A} (= z\text{-axis} \cup \{\infty\})$ will be notation for our braid axis, and $\{H_\theta | 0 \leq \theta < 2\pi\}$ will be our collection of disc that make up \mathbf{H} , our braid fibration.

For a closed n -braid $X \subset \mathbb{R}^3 \setminus \{z\text{-axis}\}$ a *rectangular block presentation* \mathcal{R}_X is a collection of disc $\{R_1, \dots, R_l\} \subset \mathbb{R}^3 \setminus \{z\text{-axis}\}$ satisfying the following conditions.

- (0) For every point $(\rho, \theta, z) \in R_i$ we have $\rho \geq 1$.
- (1) For each R_i we have $\partial R_i = r_i^1 \cup r_i^2 \cup r_i^3 \cup r_i^4$ where:
 - (a) $r_i^1 \subset H_{\theta_i^1}$ and $r_i^3 \subset H_{\theta_i^3}$ for $H_{\theta_i^1}, H_{\theta_i^3} \in \mathbf{H}$ with $\theta_i^1 < \theta_i^3$. (That is, r_i^1 is the *bottom side* and r_i^3 is the *top side* of R_i in the \mathbf{H} fibration.)
 - (b) $r_i^2 \subset P_{z_i^2} \cap \mathcal{T}_1$ and $r_i^4 \subset P_{z_i^4} \cap \mathcal{T}_1$.
- (2) Still appealing to the specified notation in condition (1), $\theta_i^1 = \theta_j^1$ iff $i = j$. Likewise, $\theta_i^3 = \theta_j^3$ iff $i = j$. Similarly, $z_i^2 = z_j^2$ iff $i = j$; and, $z_i^4 = z_j^4$ iff $i = j$.
- (3) There exists a fixed integer $0 \leq k \leq l$ such that if $\theta_i^4 = \theta_j^1$ then $i + k = j \pmod l$. In particular, $r_i^4, r_{i+k}^1 \subset H_{\theta_i^4} (= H_{\theta_{i+k}^1})$.

- (4) $r_i^2 \cap r_j^4 \neq \emptyset$ then $i = j + 1$. In particular, $z_{i+1}^2 = z_i^4 \pmod{l}$.
- (5) The leaves of the induced foliation of each R_i are arcs parallel to the r_i^1 side (or, equivalently the r_i^3 side). Thus, each leaf of $\mathcal{R}_X = \cup_{1 \leq i \leq l} R_i$ is also an arc.
- (6) By a braid isotopy of X in $\mathbb{R}^3 \setminus \{z\text{-axis}\}$ we can position it so as to have $X \subset \cup_{1 \leq i \leq l} R_i (= \mathcal{R}_X)$ such that X transversely intersects each leaf in the foliation of \mathcal{R}_X exactly once. (Thus, X is a deformation retract of \mathcal{R}_X , the retraction occurring along leaves of \mathcal{R}_X foliation.)

Rectangular block presentations of any given closed n -braid are readily produced. Referring ahead Figure 5 if the reader only focuses on the rectangular blue blocks then one has a local portion of a possible rectangular block presentation with $k = 1$. More specifically, again just focusing on the blue blocks, in Figure 14 one has a rectangular block presentation of the positive trefoil.

We say that a rectangular block presentation \mathcal{R}_X has *homogeneous twisting* if for any triple $(z_{i-1}^4, z_i^4, z_{i+1}^4)$ satisfying the condition that $z_{i+1}^4 < z_{i-1}^4 < z_i^4$ then we have that $z_{i+1}^4 < z_{i+2}^4 < z_i^4$. (Similarly, if $z_i^4 < z_{i-1}^4 < z_{i+1}^4$ then we have that $z_i^4 < z_{i+2}^4 < z_{i+1}^4$.) In §5 we show how rectangular block presentations having homogeneous twisting of any n -braid are readily produced. The rectangular block presentation of the positive trefoil in Figure 14 is such a presentation.

Now we introduce a concept that is more restrictive on rectangular block presentations. Given \mathcal{R}_X , as we traverse the copy of X it contains we will cross the leaves that contain the r_i^1 and r_i^3 sides of R_i 's. Our notation for this finite sequence of arc leaves will be $\{\lambda_1, \dots, \lambda_l\} \subset \mathcal{R}_X$ (where the index indicates the cyclic order of intersection with X). By our conditions on \mathcal{R}_X , λ_i will: intersect $k + 1$ blocks; contain r_i^4 and r_{i+k}^1 (or, flipping things around, r_i^1 and r_{i+k}^4 ; and, $\lambda_i \cap \mathcal{T}_1$ will be $3 + k$ points $\{\varrho_i(1), \dots, \varrho_i(3 + k)\}$.

We say that a rectangular block presentation \mathcal{R}_X is *interlocking* if for every consecutive pair of leaves $(\lambda_j, \lambda_{j+1})$ there exists a sub-collection of leaves $\{\lambda_{u_j^1}, \dots, \lambda_{u_j^v}\}$ such that:

- (i) For disc fibers of \mathbf{H} , $\lambda_j \subset H_{\theta_j}$, $\lambda_{u_j^1} \subset H_{\theta_j^1}, \dots, \lambda_{u_j^v} \subset H_{\theta_j^v}$, $\lambda_{j+1} \subset H_{\theta_{j+1}}$, we have that the angular order being $\theta_j < \theta_j^1 < \dots < \theta_j^v < \theta_{j+1}$.
- (ii) The endpoint $\varrho_{u_j^1}(3 + k) \in \lambda_{u_j^1}$ has z -coordinate between the endpoints $\varrho_j(1)$ & $\varrho_j(2)$ of λ_j .

- (iii) Iteratively, the endpoint $\varrho_{u_j^{w+1}}(3+k) \in \lambda_{u_j^{w+1}}$ has z -coordinate between the endpoints $\varrho_{u_j^w}(1)$ & $\varrho_{u_j^w}(2)$ of $\lambda_{u_j^w}$.
- (iv) Finally, the endpoint $\varrho_{u_j^v}(3+k) \in \lambda_{u_j^v}$ has z -coordinate between the endpoints $\varrho_{j+1}(3+k-1)$ & $\varrho_{j+1}(3+k)$ of λ_{j+1} .

Not all closed n -braids have interlocking rectangular block presentations. For example, we state without proof the the unknot does not have such a presentation. (Once the naturality of interlocking is understood this claim can be see as a corollary of Theorem 1 [M2].) Again, focusing only on the blue rectangular blocks in Figure 14, it is readily observed that the rectangular block presentation of the positive trefoil has homogeneous twisting and is interlocking. (The intuition behind the concept of an interlocking presentation should be self-evident: if we try to push r_j^3 forward in \mathbf{H} to slide past r_{j+1}^1 we are forced to push $\lambda_{u_j^1}$ forward, which pushes $\lambda_{u_j^2}$, which pushes, etc; until we are forced to push λ_{j+1} forward.)

We can now state the main result in this paper.

Theorem 1 *Every cable knot is either exchange reducible or through a sequence of braid isotopies, exchange moves and \pm -destabilizations reducible to an iterated cabling of a braid that admits an interlocking homogeneous twisting rectangular block presentation. (This secondary braid is necessarily also a cable knot.) Torus knots, in particular, are exchange reducible.*

The ending observation, that torus knots are exchange reducible, immediately implies the result of [M2], torus knots are transversally simple.

To state this result in a more exacting manner, it is useful to recall our notational machinery from [M1]. Let $\mathcal{T}_{\mathcal{C}} \subset S^3$ be a peripheral torus for an oriented knot $\mathcal{C} \subset S^3$. The oriented simple closed curve on $\mathcal{T}_{\mathcal{C}}$ that represents the homotopy class of $pm + ql$, where m is the meridian homotopy class, l is the preferred longitude homotopy class and $p, q \in \mathbb{Z}$, is called the (p, q) cable of \mathcal{C} . (Since the closed curve is necessarily of one component, p and q are relatively prime.) We used the notion $\mathbf{C}(\mathcal{C}, (p, q))$ to indicate the resulting oriented knot of this *cabling operation*.

Now, an iterated torus knot is obtained by taking the initial knot \mathcal{C}_0 as the oriented unknot. Specifically, we take sequence of co-prime 2-tuples of integers $(P, Q) = \{(p_1, q_1), (p_2, q_2), \dots, (p_h, q_h)\}$, and we can construct the oriented knot

$$K_{(P,Q)} = \mathbf{C}(\mathbf{C}(\dots \mathbf{C}(\mathbf{C}(\mathcal{C}_0, (p_1, q_1)), (p_2, q_2)) \dots, (p_{h-1}, q_{h-1})), (p_h, q_h)).$$

Theorem 1 can then be view as saying any $K_{(P,Q)}$ is either exchange reducible or there is a proper subsequence of (P, Q) , $(P', Q') = \{(p_1, q_1), \dots, (p_{h'}, q_{h'})\}$ such that $K_{(P',Q')}$ admits an interlocking homogeneous twisting rectangular block presentation.

The outline of this note is as follows. In §2 we detail the error in the analysis of standardly tiled cabling tori that lead to the flaw in the proof of Theorem 1.1 of [M2]. Once there is a sufficient understanding of the corrupting error we go on to prove that all torus knots are exchange reducible. In §3 we continue our analysis of the standardly tiled tori that carry $K_{(P,Q)}$. This will allow us to then give the proof of Theorem 1.

In §5 we give a procedure for constructing interlocking homogeneous twisting rectangular block presentations. Such presentations have applications in the study of transversal and Legendrian knots in the standard contact structure for \mathbb{R}^3 or S^3 . In particular, in the §6-Appendix (joint with H. Matsuda) we will discuss the explicit representations to the $(2, 3)$ cabling of the $(2, 3)$ torus knot (the positive trefoil) that was implicitly discovered in Theorem 1.7 of [EH]. The utilized rectangular block presentation was first discovered V. Pinciu [P] and are further exploited in [C, D].

We remark that with the availability of manuscripts on-line it makes sense to make use of color in figures that can be viewed on a computer screen in spite of the fact that color is not as widely available in print. Thus, color labeling the different salient features of a number of figures will be utilized in this note. Where possible we will also employ the redundancy of symbolic labeling.

2 Understanding the error in Theorem 1.1 and exchange reducible for torus knots

Before we describe the error in Theorem 1.1 of [M2] we briefly review our notation. The triple (K, \mathcal{T}_C, m) is comprised of an oriented cable knot K that is a curve on the torus $\mathcal{T}_C \subset S^3$ having a meridian meridian curve m . The quadruple $(K, \mathcal{T}_C, m, \Delta_m)$ is a triple with the addition of 2-disc Δ_m satisfying $m = \mathcal{T}_C \cap \Delta_m$. When **bb**-tiles are the only tiles in the singular foliation on \mathcal{T}_C , the tiling determines the four graphs $G_{\delta, \epsilon}$, $(\delta, \epsilon) \in \{(+, +), (+, -), (-, +), (-, -)\}$. Moreover, when \mathcal{T}_C has a **bb**-tiling the \mathcal{S}_K denotes the **b**-support of K in \mathcal{T}_C , the closure of the union of all the **b**-arcs that K intersects. Similarly, \mathcal{S}_m denotes the **b**-support of the meridian curve m .

The error occurs in Lemma 5.13[M1]. In particular, the alteration from Figure 15b[M1] to 16b[M1] is not valid due to an obstruction which we will describe shortly. Picking up the argument at Lemma 5.13[M1], we have established in Propositions 5.5[M1] through 5.10[M1] and Lemma 5.11[M1] that:

- All of the components of our graphs $G_{\delta,\epsilon}$ are homeomorphic to S^1 on \mathcal{T}_C .
- K coherently intersects components of $G_{\delta,\epsilon}$.
- \mathcal{S}_K is either an annulus having one boundary component from $G_{\delta,\epsilon}$ and one from $G_{-\delta,-\epsilon}$; or it is a torus-minus-a-disc having its single boundary curve being a union of four arcs, one arc coming from each of the four graphs $G_{\delta,\epsilon}$.
- The meridian curve m intersects each component of the four graphs $G_{\delta,\epsilon}$ and intersects them coherently.
- The intersection $\mathcal{S}_K \cap \mathcal{S}_m$ is a disjoint union of **b**-rectangles, rectangular regions in the foliation that is the closure of the union of all the **bb**-arcs in a single homotopic family.

To help with the visualization of the foliation of \mathcal{T}_C and \mathcal{S}_K we refer to the result in [N] from which we know that the foliation \mathcal{T}_C has a *staircase pattern* as illustrated in Figure 2. Specifically, by cutting open the foliation of \mathcal{T}_C along two edge-paths there are the union of **b**-arcs, one resembling the steps of a staircase and the other a straight path, we can place flat on a plane a fundamental region of \mathcal{T}_C .

The proof of Lemma 5.13[M1] employed the use of “non-standard” change of fibration that is illustrated in Figures 15 & 16[M1]. Specifically, an arc $\gamma \subset \partial S_m$ that in the foliation of S_m is adjacent to a single vertex (depicted as v_+ in Figure 15a[M1]) and crosses in succession a negative singular leaf followed by a positive singular leaf (depicted as s_{i+1} in Figure 15b[M1]). It is useful to complement the illustration in Figure 15[M1] with the corresponding H_θ -sequence. In Figure 3 we illustrate this sequence. The salient feature of this sequence is that the **a**-arcs adjacent to v_+ and having endpoints on γ “block” the occurrence of any singularity between the disc fibers in Figure 3b and 3d that would act as an obstruction to reversing to order of occurrence of the singularities in 3b and 3d. Thus, this portion of our erroneous argument was correct. (When we more thoroughly analyze the geometry of \mathcal{T}_C in §3 we will refer back to Figure 3.)

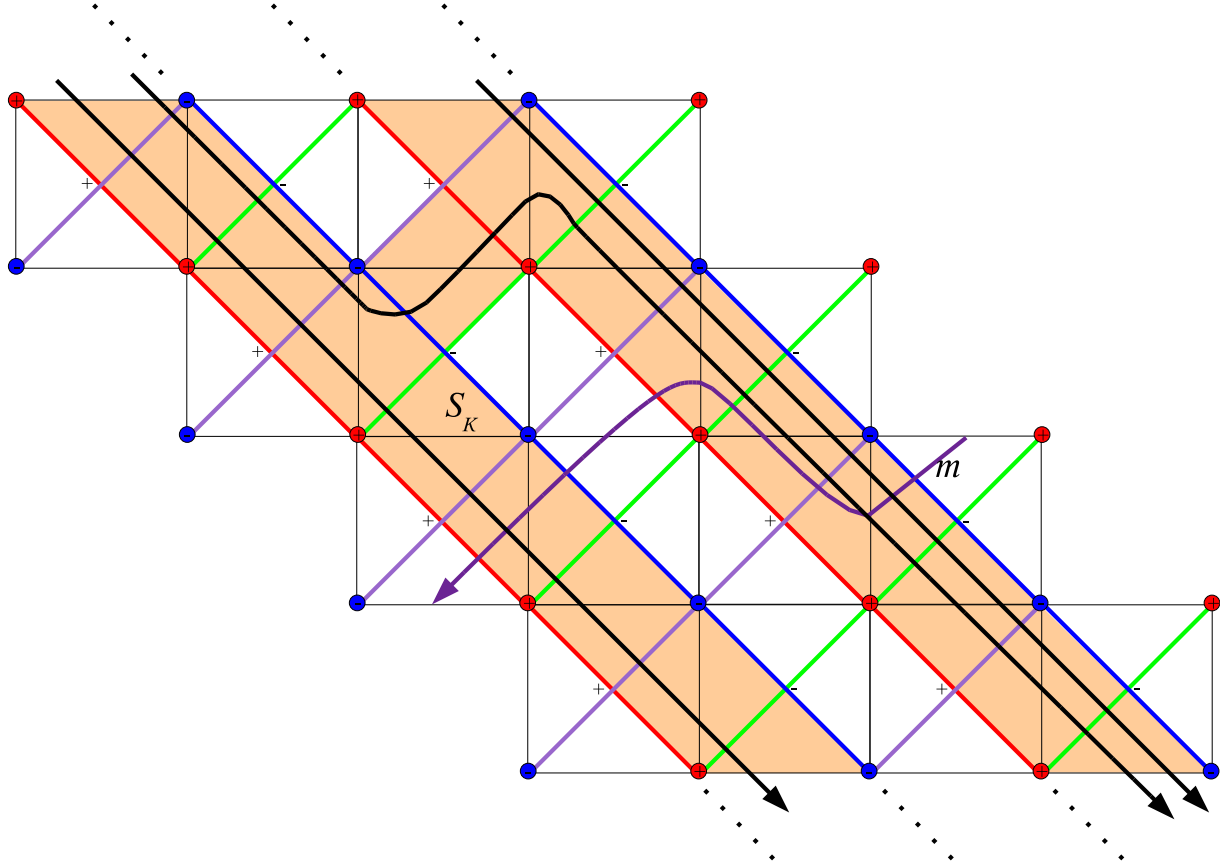


Figure 2: We depict the staircase pattern for the foliation of \mathcal{T}_C and color code the four graphs of its foliation: positive vertices are labeled $+$ and are coded **red**; negative vertices are labeled $-$ and coded **blue**; edges in $G_{+,+}$ are coded **red**; edges in $G_{-,-}$ are coded **blue**; edges in $G_{-,+}$ are coded **light magenta**; and edges in $G_{+,-}$ are coded **green**. We will always depict the meridian curves as **dark magenta** and X as **black**. Thus, are color code for the graphs is: $G_{+,+}$; $G_{-,-}$; $G_{+,-}$; and $G_{-,+}$. The **b**-support, \mathcal{S}_K is colored **light orange**.

However, there is an obstruction that can possible prevent the alteration from Figure 15b to 16b[M1] comes from the placement of K in the foliation of \mathcal{T}_C . As illustrated in Figure 4, when K is positioned in the foliation of \mathcal{T}_C so that it transversely intersects m in an “essential” manner between the singularities s_i and s_{i+1} , after the alteration to Figure 16b[M1] is performed K may no longer be transverse to the foliation and, thus, no longer positioned as a braid in the fibration \mathbf{H} . In other words, the arc $\gamma \subset m$ which we would hope to use for a non-standard change of fibration is invalid since it also intersects **b**-support of K in \mathcal{T}_C .

The question then becomes when is such an obstruction unavoidable? To answer this we revisit Proposition 5.8[M1] which governs the behavior of \mathcal{S}_K , the **b**-support

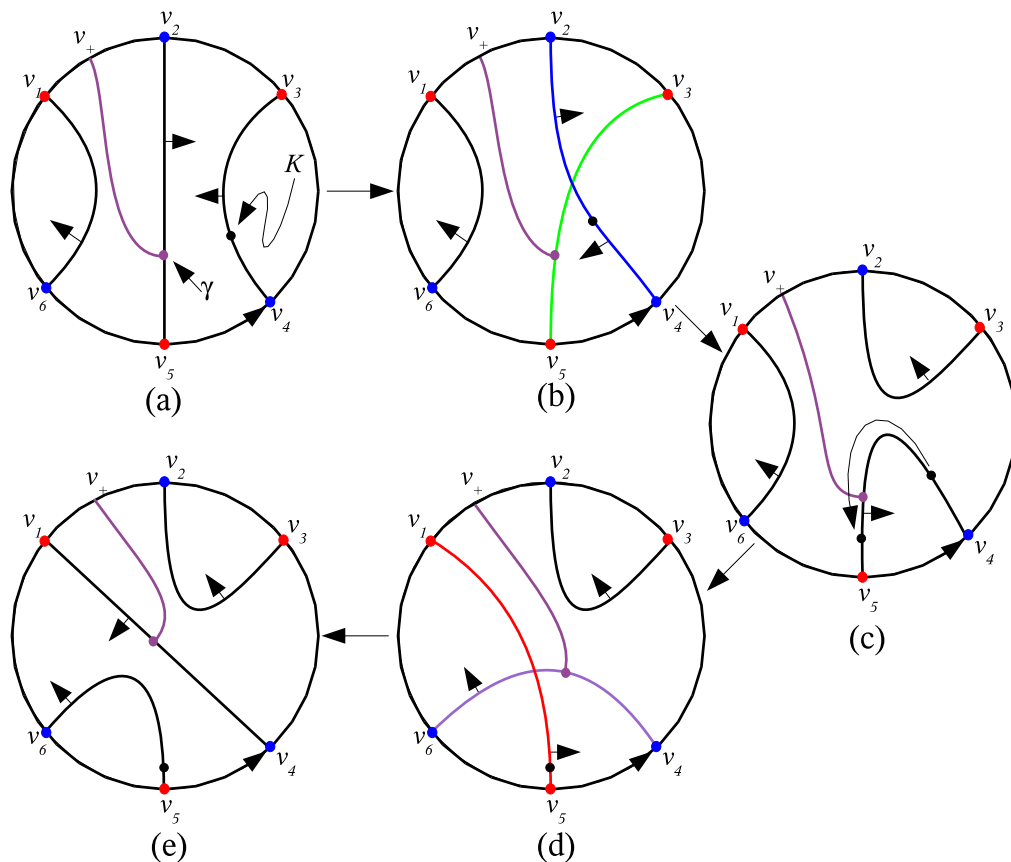


Figure 3: In (b) and (d) we have negative and positive singular leaves, respectively. Between the singularities in (b) and (d) the \mathbf{a} -arcs adjacent to v_+ “block” any other singularity occurrence from obstructing a change of fibration that would allow us to first do the positive singularity first then the negative singularity.

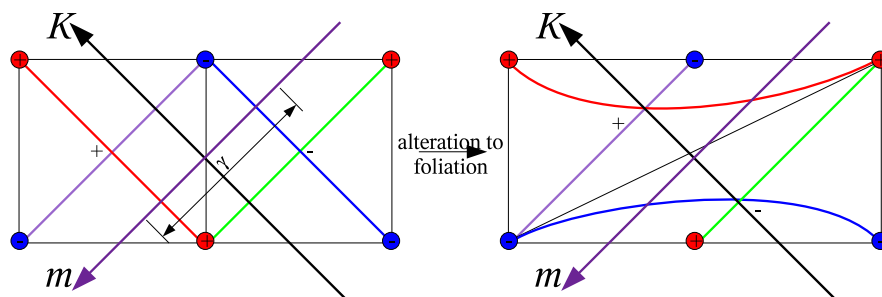


Figure 4: The left illustration depicts the knot K and the portion of the meridian curve $\gamma \subset m$ intersecting essentially. Thus, when we alter the foliation as depicted in Figure 16b[M1] K is no longer transverse to the leaves of the foliation of \mathcal{T}_C .

of K . By Proposition 5.8[M1] \mathcal{S}_K is topologically either an annulus or a torus minus an open disc.

When \mathcal{S}_K is topologically an annulus then, by Proposition 5.8(i)[M1], K is in fact parallel in \mathcal{T}_C to a component of $G_{\epsilon,\delta}$ for some ϵ, δ pair. (Equivalently, K will also be parallel to $G_{-\epsilon,-\delta}$.) Thus, for an obstruction to the alteration in the foliation as depicted in Figure 16b[M1] to be unavoidable the arc γ in Figure 15b[M1] must always be parallel in the foliation of \mathcal{T}_C to a component of $G_{-\epsilon,\delta}$ (or, equivalently, $G_{\epsilon,-\delta}$).

To see when γ is always parallel to a component of $G_{-\epsilon,\delta}$ we start with the valence one vertex depicted in Figure 16a[M1] and work backwards. In Figure 16a[M1] comes from the existence of a valence two vertex near the meridian boundary curve m that is adjacent to two singularities of common parity as depicted in Figure 15a[M1]. But, by the discussion associated with Figure 14[M1] such valence two vertices are forced to exist. Briefly summarizing that discussion, for Δ_m to be geometrically realizable m must transversally intersect $G_{\epsilon,\delta}$ for all four possible pairs of ϵ, δ . Moreover, in cyclic sequence m intersects in an alternating fashion $G_{+,+}$ and $G_{-,-}$; then m intersects in an alternating fashion $G_{+,-}$ and $G_{-,+}$. Now if m intersects any $G_{+,+}$ and $G_{+,-}$ more than once (equivalently, $G_{-,-}$ and $G_{-,+}$) then there will exist valence two vertices adjacent to singularities of either parity; and, thus, we will be able to choose γ arcs parallel to the desired $G_{\epsilon,\delta}$ graph so as to avoid an obstruction to the alteration in the foliation. We conclude that the obstruction is unavoidable exactly when m intersects either $G_{+,+}$ and $G_{-,-}$ once; or $G_{+,-}$ and $G_{-,+}$ once. (We will refer back to this as *observation-**.) Moreover, since every possible $\gamma \subset m$ must encounter \mathcal{S}_K so as to create an obstruction we can conclude that $\partial\mathcal{S}_K = G_{\epsilon,\delta} \cup G_{-\epsilon,-\delta}$ for some ϵ, δ pair, i.e. $G_{\epsilon,\delta}$ and $G_{-\epsilon,-\delta}$ have exactly one component which is topologically an S^1 .

In the case where \mathcal{S}_K is a torus minus an open disc we have a similar analysis. To start it is useful to notice that Proposition 5.8(ii)[M1] implies the \mathcal{S}_K contains a component of $\mathcal{T}_C \setminus (G_{\epsilon,\delta} \cup G_{-\epsilon,-\delta})$ for some ϵ, δ . Next, to insure that all possible $\gamma \subset m$ encounter an obstruction (as in the case of \mathcal{S}_K being an annulus) for this designated ϵ, δ pair, $G_{\epsilon,\delta}$ and $G_{-\epsilon,-\delta}$ both must be topologically S^1 and, thus, $\mathcal{T}_C \setminus (G_{\epsilon,\delta} \cup G_{-\epsilon,-\delta})$ can only have two components. We conclude again that the obstruction is unavoidable exactly when m intersects either $G_{+,+}$ and $G_{-,-}$ once; or $G_{+,-}$ and $G_{-,+}$ once. Moreover, \mathcal{S}_K intersect all outer-most **b**-arcs of \mathcal{T}_C by Lemma 2.2[M1]. (Again, we will refer back to this as *observation-**.)

We will continue this analysis in §3. But, we are now in a position to establish that torus knots are exchange reducible, the concluding statement of Theorem 1.

2.1 Torus knots are exchange reducible

We begin the argument with a brief review of the flow of the argument in [M1]. The cases of when the torus \mathcal{T}_C has a circular or mixed foliation are still established, since error in Lemma 5.13[M1] did not disturb these results. The remaining case is still when \mathcal{T}_C has tiled foliation.

As analyzed in §2, there can exist an avoidable obstruction to performing the alternation to the Figure 16[M1], since K is by assumption a torus knot $\mathcal{T}_C \subset S^3$ is an unknotted torus. Thus, we have available “meridian disc” on both sides of \mathcal{T}_C in S^3 . Let $m^i \subset \mathcal{T}_C$ correspond to the *inner meridian curve* of §5.2[M1]; and designate $m^o \subset \mathcal{T}_C$ as the *outer meridian curve*. (It may be helpful to think of m^i as a meridian curve of the unknotted core of the solid torus \mathcal{T}_C bounds, and m^o is a preferred longitude of the unknotted core.) When viewing m^o in the foliation of \mathcal{T}_C we can apply the conclusions of Proposition 5.5, 5.8, 5.9 & 5.10[M1].

Continuing let Δ_{m^o} be a disc that m^o bounds. Our tactic is to now use Δ_{m^o} to produce a non-obstructed Figure 16[M1] type alteration to the foliation of \mathcal{T}_C . With this in mind we adapt Lemma 5.11[M1] to control the foliation of Δ_{m^o} . Thus, we have the following lemma.

Lemma 2 *Let $(K, \mathcal{T}_C, m, \Delta_{m^o})$ be a quadruple where the triple (K, \mathcal{T}_C, m^o) satisfies the conclusions of Propositions 5.5, 5.8, 5.9 and 5.10[M1]. Assume there is a ϵ, δ pairing such that the inner meridian curve $m^i \subset \mathcal{T}_C$ intersects components of $G_{\epsilon, \delta}$ & $G_{-\epsilon, -\delta}$ some number of times but only intersects $G_{-\epsilon, \delta}$ & $G_{\epsilon, -\delta}$ once each. We can then assume that the initial foliation of the spanning disc Δ_m^o satisfies the following conditions:*

- (a) *There are only **ab**- & **bb**-singularities.*
- (b) *The loop $l \subset \Delta_{m^o}$ that is parallel to m^o and contains all of the positive vertices adjacent to m^o plus all of the **ab**-singularities is the union of an edge-path in $G_{+,+} \subset \Delta_m^o$ and an edge-path in $G_{+,-} \subset \Delta_m$.*

- (c) Either $G_{-,-} \cap \Delta_{m^o}$ or $G_{-,+} \cap \Delta_{m^o}$ contains an edge-path that starts and ends on m^o .
- (d) The outer meridian curve $m^o \subset \mathcal{T}_C$ intersects components of $G_{-\epsilon,\delta}$ & $G_{\epsilon,-\delta}$ some number of times but only intersects $G_{\epsilon,\delta}$ & $G_{-\epsilon,-\delta}$ once.

Proof. The argument is essentially a repeat of the argument in Lemma 4.11[M1]. Given any Δ_{m^o} we can construct a new spanning disc Δ'_{m^o} by extending Δ_{m^o} along an annulus as depicted in Figure 13[M1]. (To briefly reiterate the argument concerning the existence of such a disc, if m^o were parallel to an component of $G_{\epsilon,\delta}$ then we will be able to construct a tiled embedded disc in S^3 that has a loop in one of its $G_{\epsilon,\delta}$ graphs, a contradiction of Lemma 3.8 of [BF].) This repeated argument gives us statements (a) & (b).

To get statement (c), assume without loss of generality, the loop l of statement (b) has at least two negative singularities. Then let $C_{-,-} \subset \Delta_{m^o}$ be a component of the graph $G_{-,-}$. Notice that $C_{-,-}$ must have an endpoint on m^o (otherwise we again get a contradiction to Lemma 3.8 of [BF]). If $C_{-,-} \cap m^o$ contains more than one point then $C_{-,-}$ will contain an edge-path that satisfies statement (c). So suppose that $C_{-,-} \cap \Delta'_{m^o}$ is exactly one point. Let $\mathcal{N}(C_{-,-})$ be a regular neighborhood of $C_{-,-}$ that is the closure of the union of all of the **a** and **b** arcs that are adjacent to the vertices contained in $C_{-,-}$. Then $\partial\mathcal{N}(C_{-,-})$ contains a component $C_{+,+} \subset G_{+,+}$ that contains both positive vertices which are adjacent to the unique **ab**-singular leaf that by assumption l intersects. Now if we take Δ_{m^o} and repeat the construction that extends it by the addition of a Figure 13[M1] annulus, this $C_{+,+}$ component will be extended to a component $C_{-,+} \subset G_{-,+}$ that has $C_{-,+} \cap m^o$ containing at least two points. (By abuse of notation we still refer to the resulting boundary curve as m^o .) Thus, statement (c) is established.

Finally, we establish statement (d) as follows. Suppose a portion of $m^o (= \partial\Delta_{m^o})$ intersects in sequence components of $G_{\epsilon,\delta}$ and $G_{-\epsilon,-\delta}$ more than once. Then by the previous construction we can produce an edge-path C in the foliation of Δ_{m^o} that is either in the graph $G_{-,-}$ or $G_{-,+}$; and begins and ends on m^o . (For convenience of expository let us assume that this edge-path is in $G_{-,-}$.) But, by construction the endpoints of such an edge-path can be positioned so as to be contained in an arc $\gamma \subset m^i (\subset \Delta_{m^i})$ as depicted in Figure 15a and 16a[M1]. The two endpoints of this edge-path in Δ_{m^o} could then be “coned” to the valence-one vertex in Figure 16a[M1]. But, this would create an extension of the disc Δ_{m^o} that contains a closed loop in

its $G_{-,-}$ graph. Again, by Lemma 3.8 of [BF] such loops cannot exist. Thus, m^o can only intersect the $G_{\epsilon,\delta}$ & $G_{-\epsilon,-\delta}$ each once. Statement (d) is now established and, thus, our lemma is proved. \diamond

We now finish our argument that torus knots are exchange reducible. The main idea is simple. Given a torus knot on \mathcal{T}_C we consider the annulus or torus-minus-a-disc \mathcal{S}_K . If every possible Figure 16a[M1] type arc $\gamma \subset m^i$ cannot be used to perform a type Figure 15b[M1] alteration to the foliation of \mathcal{T}_C , it is because γ essentially intersects K in \mathcal{S}_K . So γ must locally cut across, say, $G_{\epsilon,\delta}$ and locally K is parallel to $G_{\epsilon,\delta}$. But, by statement (d) of Lemma 2 m^o will be locally parallel to $G_{\epsilon,\delta}$. We can then use the edge-path in statement (c) of Lemma 2 to produce, after a sequence of exchange move and change of fibrations, a valence-one vertex as depicted in Figure 16a[M1] (except it will be in the resultant foliation of Δ_{m^o}). Since the γ in m^o will locally be either parallel to K or not in \mathcal{S}_K , we can perform the alteration to the foliation of \mathcal{T}_C that is depicted in \mathcal{T}_C .

3 Continued analysis of standardly tiled tori and proof of Theorem 1

We now continue our analysis of the standard tiling \mathcal{T}_C of the cabling torus that in a neighborhood of \mathcal{S}_K carries $K_{(P,Q)}$. Our goal in this section is achieving a total understanding of the embedding of such cabling torus in S^3 .

The key to this understanding is based upon an understanding of the meridian curves of \mathcal{T}_C . From the analysis in [M1], and now §2, we know that all of the singularities in the foliation of Δ_m adjacent to the boundary curve m are of the same parity except for one singularity, e.g. see Figure 14a[M1]. It is convenient to assume the case where $\partial\mathcal{S}_K$ is equal to either $G_{+,+} \cup G_{-,-}$ (in the case where we have an annulus), or $\{\text{edge} - \text{path of } G_{+,+}\} \cup \{\text{edge} - \text{path of } G_{-,-}\} \cup \{\text{edge of } G_{+,-}\} \cup \{\text{edge of } G_{-,+}\}$ (in the case where we have a torus-minus-disc). (Figure 2 incorporates this assumption.) This implies that as we can position m so that it has a *simply zig-zag loop*: that is, as we traverse m it alternates between intersecting $G_{+,+}$ and $G_{-,-}$; and it intersects both $G_{+,-}$ and $G_{-,+}$ once. (Again, see Figure 2.) Observe that since m as simply zig-zag loop is transversely intersects the leaves of \mathcal{T}_C then m is a braid representation of the unknot in the fibration \mathbf{H} .

In order to help the reader visualize our ultimate goal it is useful to momentarily put aside our foliation machinery for \mathcal{T}_C and give a description of how a cabling torus in S^3 can be embedded. (We will establish in Theorem 4 that our description here is in fact the general case.)

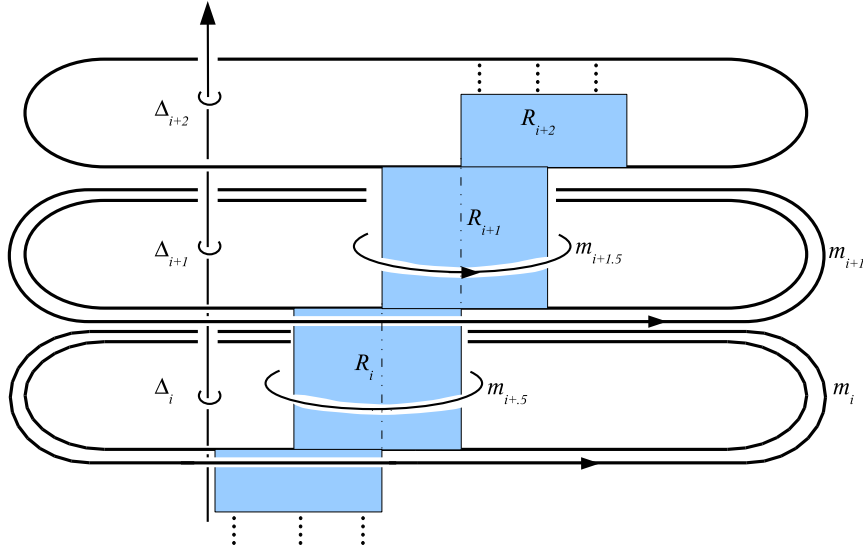


Figure 5: The steps configuration has the R_i rectangles arranged so that each “step” has a Δ_i attached. The boundary of a regular neighborhood of a steps configuration is a standard cabling torus. The illustration depicts curves $m_{i+0.5}$, m_{i+1} and $m_{i+1.5}$ which are meridian curves on the standard cabling torus. (The standard cabling torus is not explicitly depicted.)

First we describe a *steps configuration*, \mathcal{R}_X^s , for a collection of radially foliated discs and rectangular discs in \mathbf{H} . Specifically, let $\{\Delta_1, \dots, \Delta_l\}$ be a collection of discs that are arranged in a braid fibration setting so that each Δ_i is punctured once by the braid axis \mathbf{A} and has its boundary curve transverse to the braid fibration \mathbf{H} . (Thus, each Δ_i is radially foliated.) Moreover, suppose that the indexing variable is such for any triple $(\Delta_i, \Delta_{i+1}, \Delta_{i+2})$ the axis \mathbf{A} cyclically intersects these discs in the same order. (We treat $\{\Delta_1, \dots, \Delta_l\}$ as a cyclic ordering of discs.) To continue our description of the stepping configuration, let $\{R_1, \dots, R_l\}$ be a collection of rectangles such that:

- (i) $\partial R_i = r_i^1 \cup r_i^2 \cup r_i^3 \cup r_i^4$.
- (ii) R_i is attached to $\partial \Delta_i$ along r_i^2 .
- (iii) R_i is attached to $\partial \Delta_{i+1}$ along r_i^4 .

- (iv) r_i^1 & r_i^3 are contained in disc fibers of \mathbf{H} with r_i^1 the *bottom side* and r_i^3 the *top side* (as understood in condition (1a) of our definition of rectangular block presentation).
- (v) The leaves of the induced foliation of R_i by \mathbf{H} are arcs that have their endpoints on r_i^2 and r_i^4 that are parallel to r_i^1 and r_i^3 .
- (vi) The set $R_1 \cup \cdots \cup R_l$ is connected and homotopic equivalent to S^1 . The associated embedding of this S^1 in \mathbb{R}^3 is a braid X .
- (vii) For some fixed integer $k > 0$ we have that r_{i+k}^1 and r_i^3 are contained in the same leaf of the induced foliation of $R_1 \cup \cdots \cup R_l$.

We refer the reader to Figure 5. The reader should take notice of the “steps” arrangement of the set $R_1 \cup \cdots \cup R_l$ and that by construction each “step” of the configuration has a Δ_i disc attached. Thus, a regular neighborhood of $(\cup_{1 \leq i \leq l} \Delta_i) \cup (\cup_{1 \leq j \leq l} \Delta_j)$ is topologically a solid torus. We will call the boundary of such a neighborhood a *standard cabling torus*. (Referring back to our exacting description of Theorem 1 immediately after the statement of Theorem 1, we are working towards showing that the peripheral torus of $K(P', Q')$ is always a standard cabling torus.) Finally, restricting to the collection of rectangles, the reader should notice that \mathcal{R}_X^s contains an underlying rectangular block presentation \mathcal{R}_X .

Although we will not appeal to the concept until §4, we say that \mathcal{R}_X^s , and its associated standard cabling torus \mathcal{T}_C , has *interlocking homogeneous twisting* if the underlying rectangular block presentation \mathcal{R}_X does.

It is readily seen that a standard cabling torus is in fact one of our tiled \mathcal{T}_C : each vertex is valence four and the parity of the tiles correspond to a checker-board pattern. Specially, we refer the reader to the definition of \mathbf{b} -support of K , \mathcal{S}_K and the statement of Proposition 5.8[M1] governing the behavior of \mathcal{S}_K . By Proposition 5.8[M1] topologically \mathcal{S}_K is either an annulus or a torus minus an open disc. In either case, by observation- \star we now know that a meridian curve transversely cuts through \mathcal{S}_K everywhere except at one place where it must intersect, say, $G_{+,-}$ and $G_{-,+}$ once. In Figure 6 we have depicted the meridian curves m_i & m_{i+1} which cut across \mathcal{S}_K several times, transversally intersecting $G_{+,+}$ and $G_{-,-}$, but only once are depicted as intersecting $G_{+,-}$ and $G_{-,+}$. The labeling of the curves m_i & m_{i+1} in Figure 6 is meant to correspond to the labeling of curves m_i & m_{i+1} in Figure 5. We ask the reader to notice that in Figure 5 all of the m -curves are isotopic to each other in

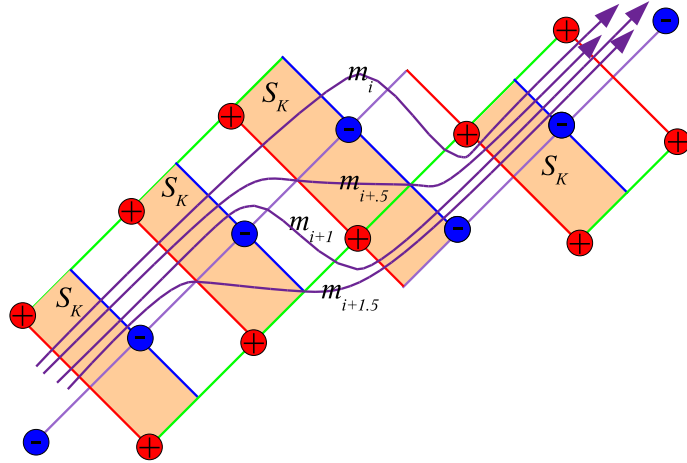


Figure 6: The tiling foliation of \mathcal{T}_C can be “laid out flat” in a staircase pattern. The limitation that m intersect exactly once $G_{+,-}$ and $G_{+,+}$ illustrated. (A choice of parity is made for the purpose of illustration simplification since there is a similar figure using $G_{-,+}$ and $G_{-,-}$.)

the complement of the standard disc-rectangle configuration, and thus are isotopic meridian curves on the standard cabling torus. Moreover, we ask the reader to see that the isotopy from m_i to m_{i+1} which has $m_{i+1.5}$ as an intermediary curve is in fact an exchange move of type-I as illustrated in Figure 11[M1]: the n -braid m_i passes through the axis \mathbf{A} to become $m_{i+1.5}$, a meridian curve that has two points of tangency with the braid fibration \mathbf{H} ; and the passes through \mathbf{A} to become the n -braid m_{i+1} . The corresponding sequence is depicted in Figure 6: The curve m_i is transverse to the foliation of \mathcal{T}_C ; the isotopy of m_i to $m_{i+1.5}$ passes through a negative vertex and $m_{i+1.5}$ intersects two singular points in the foliation—points where $m_{i+1.5}$ is necessarily tangent to disc fibers of \mathbf{H} ; and, finally $m_{i+1.5}$ passes through a position vertex to become m_{i+1} which is transverse to the foliation of \mathcal{T}_C . Iterating this isotopy on the new n -braid m_{i+1} we can swipe out the entire foliation of \mathcal{T}_C until we arrive back at m_i .

As previously stated, our goal is to show that all the \mathcal{T}_C of any triple (K, \mathcal{T}_C, m) is a standard cabling torus. In order to show this it is sufficient to show that there is a meridian curve m_i satisfying observation- \star that is a 1-braid with respect to \mathbf{A} . Thus, we have the following proposition.

Proposition 3 *Let $m \subset \mathcal{T}_C$ be a meridian curve position as a simply zig-zag loop. Assume that m intersects $2s$ singular leaves in the foliation of \mathcal{T}_C . Then the braid index of m is either 1 or $s - 1$.*

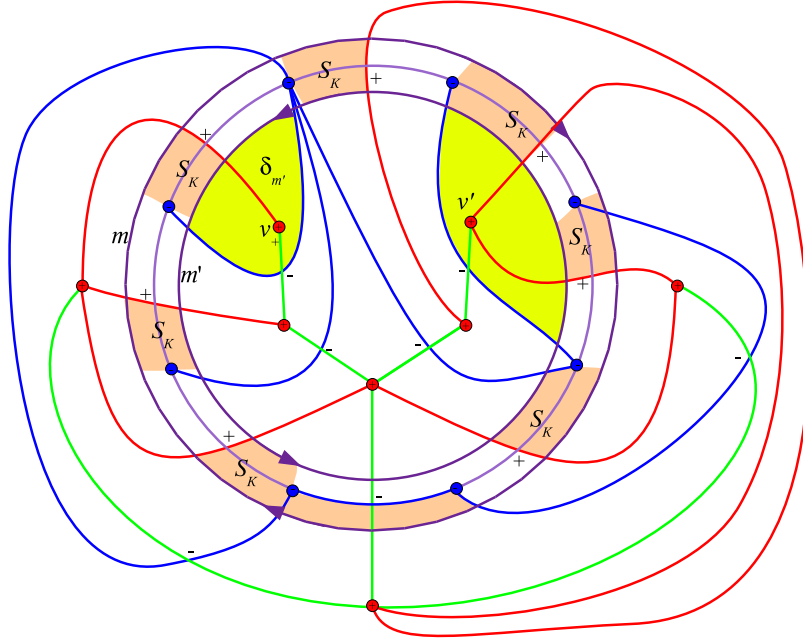


Figure 7: The meridian curves m & m' are simply zig-zag loops when viewed in the foliation of \mathcal{T}_C , and they co-bound an annulus $\mathcal{A} \subset \mathcal{T}_C$ as illustrated. The portion of $\mathcal{S}_K \cap \mathcal{A} \subset \mathcal{A}$ is indicated by the shaded regions above. Attached to \mathcal{A} along its boundary curves are the two meridian discs Δ_m & $\Delta_{m'}$. A sub-disc $\delta_{m'} \subset \Delta_{m'}$ has $\partial\delta_{m'} = \alpha_1 \cup \alpha_2$ where $\alpha_1 \subset m'$ & $\alpha_2 \subset G_{-,-}$; and $\delta_{m'}$ contains exactly one vertex of v_+ which is an endpoint of $G_{+,+}$. The vertex v' illustrates an opportunity for a non-standard change of fibration.

Proof. We start by considering two parallel meridian curves, $m, m' \subset \mathcal{T}_C$, which co-bound a sub-annulus $\mathcal{A} \subset \mathcal{T}_C$ which has an induced foliation that contains only negative vertices of \mathcal{T}_C . (See Figure 7 and its caption description.) To elaborate further, the foliation of \mathcal{T}_C restricted to \mathcal{A} will have s positive vertices and s singular points. Since m & m' are simply zig-zag loops all but one of these singular points will have positive parity.

We now use that fact that m and m' both bound meridian discs in \mathcal{T}_C to extend \mathcal{A} to a 2-sphere. Let Δ_m and $\Delta_{m'}$ be meridian disc in \mathcal{T}_C having having m and m' as boundary curves, respectively. Then $\Sigma = \Delta_m \cup \mathcal{A} \cup \Delta_{m'}$ is a 2-sphere. As previously noted, the foliations of Δ_m and $\Delta_{m'}$ will only positive vertices in their foliation, i.e. all of the negative vertices live in \mathcal{A} .

With this setup we start our argument with the claim that in $\Delta_{m'}$ there exists a sub-disc $\delta_{m'}$ such that: $\partial\delta_{m'} = \alpha_1 \cup \alpha_2$ where $\alpha_1 \subset m'$ & α_2 is in the $G_{-,-}$ graph of $\delta_{m'}$; and, $\delta_{m'}$ contains exactly one vertex of the $G_{+,+}$ (of $\Delta_{m'}$) which is an endpoint

of $G_{+,+}$. The arc α_2 is necessarily then contained in a negative singular leaf of the foliation of Σ and α_1 must have angular length 2π in \mathbf{H} . To see this first notice that by construction Σ' 's $G_{-,+}$ graph is totally contained in \mathcal{A} ; and, its $G_{+,-}$ graph must then intersect \mathcal{A} in exactly one arc that cuts through the single negative singularity contained in \mathcal{A} . Since all of Σ' 's $G_{\epsilon,\delta}$ graphs must be simply connected (a property of such graphs on 2-spheres following again from Lemma 3.8 of [BF]), we have $\Delta_{m'}$ containing an endpoint of $G_{-,+}$ which we label v_+ . If v_+ is the only positive vertex in $\Delta_{m'}$ then from v_+ we can see m' in sequence: intersects $G_{+,+}$; pass through \mathcal{S}_K ; intersects $G_{-,-}$; and, finally, an intersection with $G_{+,+}$. Thus, we can perform a non-standard change of fibration between the middle $G_{-,-}$ singularity and the last $G_{+,+}$ singularity. So assume that $\Delta_{m'}$ contains more than one positive vertex. Now again suppose that v_+ is adjacent to more than one edge of $G_{+,+}$. This again would imply that from the vertex v_+ we can see in sequence: intersects $G_{+,+}$; pass through \mathcal{S}_K ; intersects $G_{-,-}$; and an intersection again with $G_{+,+}$. But, this again would give us the ability to perform a non-standard change of fibration to alter the foliation of \mathcal{T}_C so as to produce valence three, then valence two vertices. (Recall valence two vertices can be eliminated using exchange moves.)

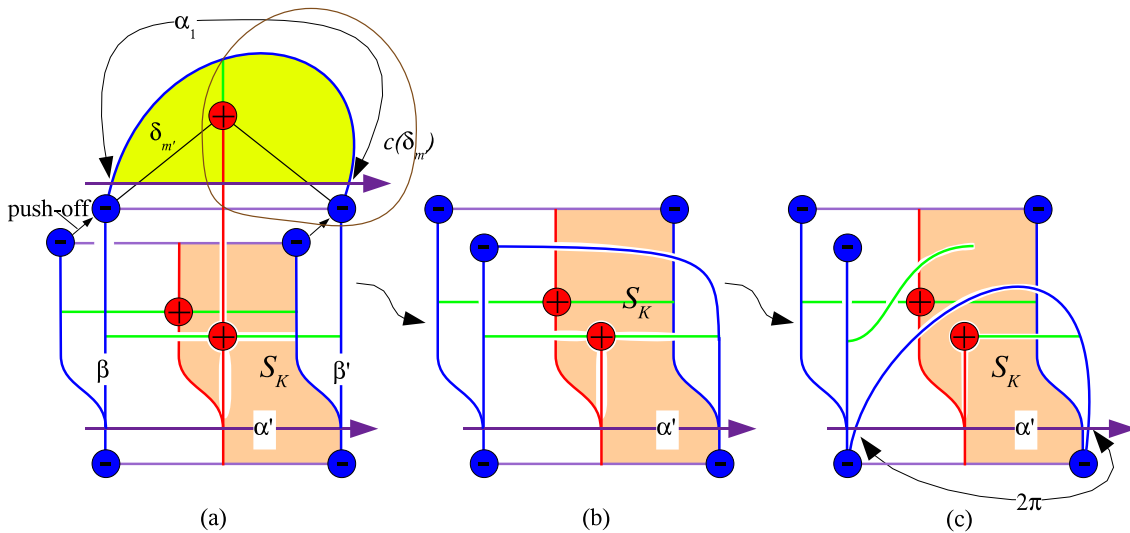


Figure 8: In the illustration the push-off of $\delta_{m'} \cup (R \setminus \alpha')$ is shown “above” the foliation of \mathcal{T}_C . In (a) we perform an exchange move predicated on the existence of the valence two vertex in $\delta_{m'}$ so that the \mathbf{b} -arcs inside the $c(\delta_{m'})$ -curve are inessential and can be eliminated to produce the foliation in (b). We go from (b) to (c) via a standard change of fibration.

So we now have an $\alpha_1 \subset m'$ that has angular length 2π and, when transversed in the direction of its orientation, intersects $G_{+,+}$, passes through \mathcal{S}_K , then intersects

$G_{-,-}$. (See Figure 8.) We now refer to Figure 8 and use its configuration to argue that as we move along \mathcal{S}_K there are arcs having similar intersection sequence that also angular length 2π . Specifically, we focus on the sub-disc $\delta_{m'}$ that is attached to \mathcal{T}_C along the arc α_1 . Let R be a rectangular region in \mathcal{T}_C such that: $\partial R = a_1 \cup \beta \cup \alpha' \cup \beta'$; both β & β' are arcs in the $G_{-,-}$ graphs of \mathcal{T}_C ; and α' is an arc whose entire is transverse to \mathcal{T}_C 's foliation and passes into \mathcal{S}_K after intersecting $G_{+,+}$ as shown in Figure 8. We now push a copy of $\delta_{m'} \cup (R \setminus \alpha')$ off into the solid torus that \mathcal{T}_C bounds in S^3 leaving $\delta_{m'} \cup R$ attached to \mathcal{T}_C along α' . (Thus, the observer's viewpoint in Figure 8 is from inside the solid torus.) We now pass from Figure 8(a) to 8(b) by performing an exchange move and an elimination of a valence two vertex. Next, we pass from Figure 8(b) to 8(c) by performing a standard change of fibration. This yields an arc in \mathcal{T}_C that is slightly shifted in the foliation (which we still call α'), and it has the intersection sequence of first hitting $G_{+,+}$, passing through \mathcal{S}_K before hitting $G_{-,-}$. Since α' intersects twice the singular leaf in what remains of the altered R its angular length must be 2π . Iterating this argument over all of \mathcal{S}_K we see that any oriented arc that is: positively transverse to the foliation of \mathcal{T}_C ; has endpoints on $G_{-,-}$; does not intersect $G_{-,+}$ or $G_{+,-}$; intersects $G_{+,+}$ before it enters the entire of \mathcal{S}_K ; and has angular length 2π . Since m' passes through \mathcal{S}_K $s - 1$ -times, its angular length is at least $2\pi(s - 1)$. But, since the braid index of $m \cup m'$ is equal to the number of vertices contained in \mathcal{A} , and since the braid index of m is at least 1, we must have that the index of m is 1 and m' is $s - 1$. \diamond

For the propose of completeness Figure 9 illustrates the foliation of a Σ -sphere that has Δ_m radially foliated and $\Delta_{m'}$ foliated with $s - 1$ positive vertices (where $s = 8$).

We are now in a position to establish our previously stated goal.

Theorem 4 *The \mathcal{T}_C of any triple (K, \mathcal{T}_C, m) is a standard cabling torus.*

Proof. We will establish that \mathcal{T}_C is a standard cabling torus by building the associated \mathcal{R}_X^s . To do this we need to specify the Δ_i -discs and the R_j -rectangles.

Let $\{m_1, \dots, m_l\}$ be a sequence of zig-zag meridian curves all of braid index one such that $m_i + 1$ is obtained from m_i via the type-I exchange move illustrated in Figure 6, and m_1 is obtained from m_l also by such a move. Then as we push m_1 to m_2 to m_3 until we arrive back at m_1 we will have sweep out our torus \mathcal{T}_C . Now let Δ_i be a meridian disc inside the solid torus that \mathcal{T}_C bounds. Since m_i is a one braid δ_i

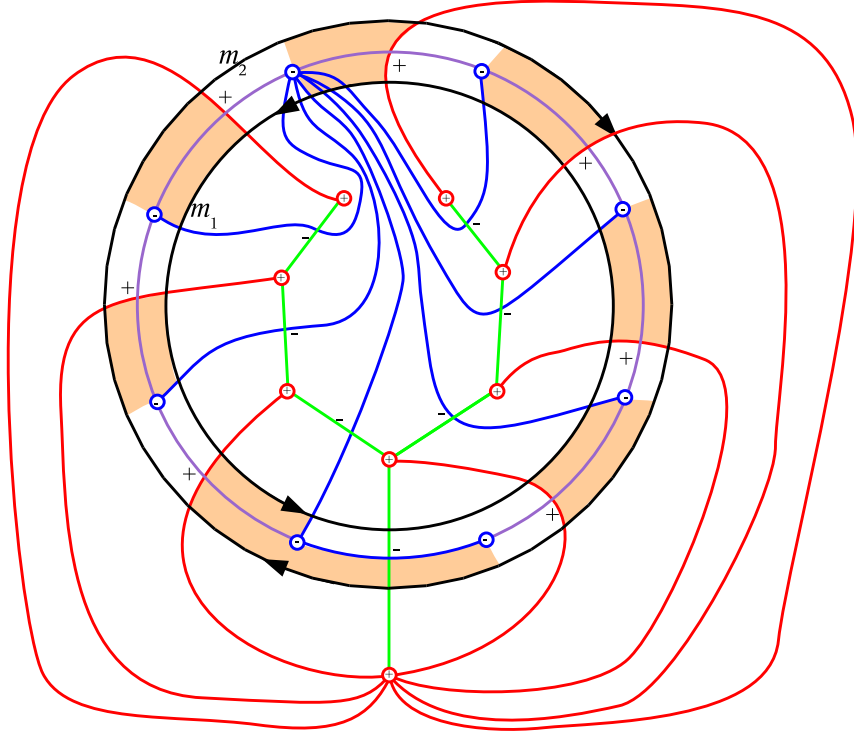


Figure 9: In this illustration the “outside” meridian disc has exactly one vertex, thus, implying that the corresponding boundary meridian curve is a 1-braid.

will be punctured algebraically once by \mathbf{A} and, thus, geometrically once by \mathbf{A} . (That is, exchange moves and the elimination of any inessential \mathbf{b} -arcs in the foliation of Δ_i will produce a radially foliated discs.) We let this collection of radially foliated discs be our radially foliated discs of our steps configuration.

It remains to describe how we can specify the rectangular discs of our needed steps configuration. But an initial collection of such rectangular discs is easily obtained from the positioning of the m_i 's in the foliation of \mathcal{T}_C . Referring to Figure 10 (which is a variation on Figure 5) we see that there is a natural region between m_i and m_{i+1} that is between the two singular leaves which $m_{i+.5}$ is tangent to. This region has an induced foliation corresponding to that of condition (v) in our description of the steps configuration. Specifically referring to the shaded region in Figure 10: $r_i^2 = R_i \cap m_i$; $r_i^4 = R_i \cap m_{i+1}$; r_i^1 is the edge-path in one of the singular leaf in ∂R_i ; and r_i^3 is the edge-path in the other singular leaf in ∂R_i . Since singular leaves are contained in disc fibers of \mathbf{H} we have the r_i^1 & r_i^3 are contained in disc fibers. By choosing r_i^1 to be associate with the negative singularity and r_i^3 associated with the positive singularity we can have r_i^1 being the bottom side and r_i^3 being the top side of our R_i rectangle.

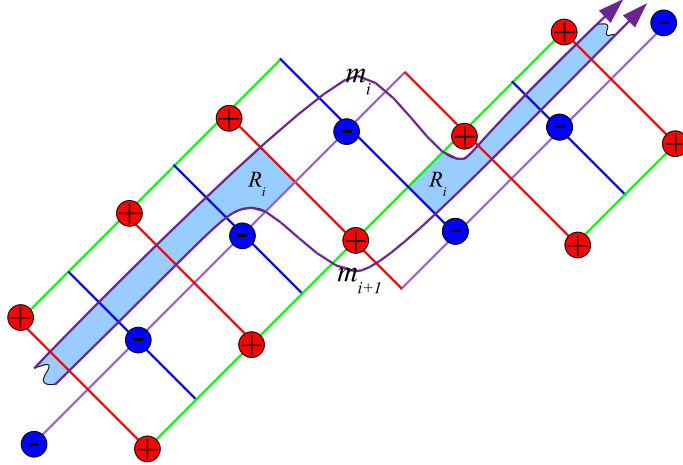


Figure 10: The shaded “rectangular” region labeled R_i is attached to m_i (resp. m_{i+1}), and thus Δ_i (resp. Δ_{i+1}). After possibly “shaving off” the two sides contained in disc fibers of $\mathbf{H} R_i$ will then correspond to the R_i in Figure 5.

So conditions (i)-(iv) of our steps configuration description are satisfied. By “shaving off” the r_i^1 and r_i^3 sides of all the R_i rectangular discs we can easily obtain condition (v). Now we notice that the union of all these R_i 's in \mathcal{T}_C is topologically an annulus so we obtain condition (vi). Condition (vii) follows from the regularity of the staircase pattern of our \mathcal{T}_C foliation in Figure 2. Specifically, the fixed k in condition (vi) is equal to $s - 2$ where $2s$ is the number of singular leaves a zig-zag meridian curve intersects in the foliation of \mathcal{T}_C . Clearly the boundary of a regular neighborhood of $\mathcal{R}_X^s = (\cup_{1 \leq i \leq l} \Delta_i) \cup (\cup_{1 \leq j \leq l} R_j)$ is again a standardly tiled torus that is isotopic to our original \mathcal{T}_C in our axis/fibration coordinate system. \diamond

4 Proof of Theorem 1

We restate the argument in [M1] up to the error in Theorem 1.1. We begin with a quadruple $(K, \mathcal{T}_C, m, \Delta_m)$. Through a sequence of exchange moves and destabilizations we can assume that \mathcal{T}_C (which contains K) has been position arbitrarily close (in the (\mathbf{A}, \mathbf{H}) coordinate system) to a knot K' that is positioned on a cabling torus \mathcal{T}'_C that has either: a circular foliation; or, a mixed foliation; or, a tiled foliation. For the first two possibilities by Corollary 3.1[M1] and Proposition 4.1[M1] we have that K is exchange reducible. For the tiled foliation case we are left with K' being positioned in the \mathbf{b} -support $\mathcal{S}_{K'} \subset \mathcal{T}'_C$ that is either an annulus or a torus-minus-a-disc,

as described in Proposition 5.8[M1]. To establish our theorem we need to show that the associated \mathcal{R}_X^s to \mathcal{T}'_C has its underlying rectangular block presentation \mathcal{R}_X having interlocking homogeneous twisting. As the reader may now suspect we will derive the needed rectangular block presentation from the tiled foliation of \mathcal{T}'_C .

So our starting point is in fact the tiled foliation of \mathcal{T}'_C . As described in the proof of Theorem 4 from the tiled foliation of \mathcal{T}'_C we can readily produce a step configuration for which the boundary of a regular neighborhood corresponds to \mathcal{T}'_C . By positioning each Δ_i disc in the configuration to be contained in an appropriate level plane P_{z_0} and scaling their radii to be 1, we can achieve the condition that all of the r_i^2 - & r_i^4 -sides of the configuration's rectangular discs are contained in \mathcal{T}'_1 . Moreover, we can then easily isotop the rectangular discs to have empty intersection with the interior of the solid cylinder that \mathcal{T}'_1 bounds in \mathbb{R}^3 . Once this positioning of the rectangular discs it is self evident that their union is a rectangular block presentation \mathcal{R}_X of the braid X which passes through each $R_i(\subset \mathcal{T}'_C)$ once and, thus, intersects each simply zig-zag meridian curve on \mathcal{T}'_C once. Clearly X is a longitude of \mathcal{T}'_C ; $\cup_{1 \leq i \leq l} R_i = \mathcal{R}_X$ is a rectangular block presentation; and K' is a cabling of X .

We now need to establish that \mathcal{R}_X has homogeneous twisting and is interlocking. The argument for each is to show that if \mathcal{R}_X does not possess the claimed property then there will exist a standard change of fibration which is not obstructed by K' that allows us to continue to simplify the foliation of \mathcal{T}'_C through braid isotopies, exchange moves and \pm -destabilizations of K' . We use two claims to organize the remaining argument.

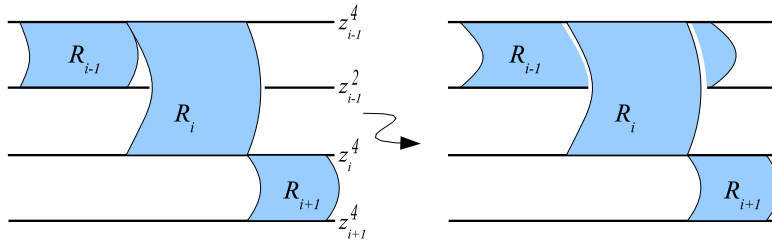


Figure 11:

Claim 1— \mathcal{R}_X has homogeneous twisting.

We refer the reader to Figure 11 for this argument. Reiterating the condition for homogeneous twisting, we require that for any triple $(z_{i-1}^4, z_i^4, z_{i+1}^2)$ satisfying the condition that $z_{i+1}^4 < z_{i-1}^4 < z_i^4$ then we have that $z_{i+1}^4 < z_{i+2}^4 < z_i^4$. Suppose this is not the case. Then either $z_{i+2}^4 < z_{i+1}^4 < z_i^4$ or $z_{i+1}^4 < z_i^4 < z_{i+2}^4$. The left-hand

side illustration in Figure 11 depicts the situation when $z_{i+1}^4 < z_{i+2}^4 < z_i^4$. We are allowing this figure to serve a dual purpose: it illustrates a portion of a rectangular block presentation \mathcal{R}_X ; and it illustrates a portion of a step configuration \mathcal{R}_X^s . When viewing a step configuration one should realize that associated with each block is a negative singularity (before the r_j^1 -side in the fibration \mathbf{H}) and a positive singularity (after the r_j^3 -side in \mathbf{H}). Now going back to our current figure, if we can “slide” the r_{i-1}^3 -side of R_{i-1} forward in \mathbf{H} along $\partial\Delta_{i-1}$ and $\partial\Delta_i$ so as to move it past the r_i^1 -side of R_i then in the corresponding tiling of $\mathcal{T}'_{\mathcal{C}}$ we will have preformed a nonstandard change of fibration to the tiling. One should observe that the braid $K' \subset \mathcal{T}'_{\mathcal{C}}$ will not act as an obstruction to such a nonstandard change in fibration since K' can be viewed as being positioned within an arbitrarily small neighborhood of the set

$$(\cup_{1 \leq i \leq l} (\partial\Delta_i)) \cup (\cup_{1 \leq i \leq l} \lambda_i) \subset (\cup_{1 \leq i \leq l} \Delta_i) \cup (\cup_{1 \leq i \leq l} R_i) \subset \mathcal{T}'_{\mathcal{C}}. \quad (1)$$

So the only possible obstruction to performing this slide will come from the positioning of the rectangular blocks themselves. However, as seen in Figure 11, the R_i block “shields” the sliding of the r_{i-1}^3 -side of the R_{i-1} block from obstruction—all of the rectangular blocks positioned “underneath” R_i can be pushed forward in \mathbf{H} before we slide r_{i-1}^3 past r_i^1 . Thus, our claim is established. (A similar illustration can be used to depict the situation where $z_{i+1}^4 < z_i^4 < z_{i+2}^4$. This argument can also be presented in a H_θ -sequence form.)

Claim 2— \mathcal{R}_X is interlocking.

The argument establishing this claim is almost a tautology. As set equation 1 specifies, whatever alteration we make to a step configuration we cannot disturb the $(\cup_{1 \leq i \leq l} (\partial\Delta_i)) \cup (\cup_{1 \leq i \leq l} \lambda_i)$ set. So if we try to forward slide the r_j^3 -side of the R_j rectangular block along $\partial\Delta_j \cup \partial\Delta_{j+1}$ past the r_{j+1}^1 -side of the R_{j+1} block the only possible obstruction will be some $r_{u_j^1}$ -side of a rectangular contained in a $\lambda_{u_j^1} (\subset \cup_{1 \leq i \leq l} R_i)$ leaf. So we can try to slide r_j^3 along with all of $\lambda_{u_j^1}$ forward and past r_{j+1}^1 . But, again we made be obstructed by another $r_{u_j^2}$ that is contained in a $\lambda_{u_j^2}$ leaf. Continuing in this manner either we can push all obstructions to pushing r_j^3 past r_{j+1}^3 or we find that $r_{j+1}^3 (\subset \lambda_{j+1}^3)$ itself is an obstruction to pushing r_j^3 past r_{j+1}^3 . It is the latter that gives us an interlocking rectangular block presentation. If we can push all of the obstruction out of the way then we can again perform a non-standard change of fibration to the tiled foliation of $\mathcal{T}'_{\mathcal{C}}$ and reduce the complexity of its foliation through a sequence of braid isotopies, exchange moves and \pm -destabilizations. this establishes

our remaining claim and ends the proof of Theorem 1. \diamond

5 Building interlocking homogeneous twisting rectangular block presentations.

In this section we will give a general procedure for building the interlocking homogeneous twisting step configuration $\mathcal{R}_{K(P,Q)}^s$ on which the knot $K_{(P,Q)}$ lives. Necessarily we will have $(P', Q') = \{(p_1, q_1), \dots, (p_{h-1}, q_{h-1})\}$ for $(P, Q) = \{(p_1, q_1), \dots, (p_h, q_h)\}$. (Our notation (P, Q) and (P', Q') is consistent with that in §1.)

This procedure is described in terms of the H_θ -sequence and can then be readily geometrically realized as a the step configuration. Next, using the geometrically realized of the step configuration we can superimpose over it a *rectangular diagram* of a *rectangular diagram* of the cable knot $K_{(P,Q)}$. Specifically, $K_{(P,Q)}$ will be comprised as an union of *horizontal arcs* contained in the unit cylinder \mathcal{T}_1 ; and *vertical arcs* contained in half-plane $H_\theta \in \mathbf{H}$ and having $\rho \geq 1$.

There is an immediate advantage to presenting $K_{(P,Q)}$ as a rectangular diagram. A rectangular diagram readily yields a transversal braid presentation and a Legendrian knot presentation of the underlying knot type in the standard symmetric contact structure of \mathbb{R}^3 , i.e. the plane field coming from the kernel of the 1-form $\alpha = dz + \rho^2 d\theta$.

In general, by slightly tilting vertical arcs and smoothing corners any rectangular diagram of a knot K can be deformed into a closed braid. Bennequin's classical result [B], that a closed braid can also be thought of a a transversal link in the standard contact structure of \mathbb{R}^3 or S^3 , gives us that after this deformation we are looking at a transversal presentation of K . The classical invariant of transversal knots, the Bennequin number, is readily computed by taking the algebraic length less the braid index. That is, $\beta(K) = \ell - n$.

Seeing how rectangular diagrams of a knot K can be thought of as Legendrian presentations is almost as straight forward. In general, a rectangular diagram can initially be associated with a piecewise Legendrian diagram: The horizontal arcs can be associated with leave segments in the characteristic foliation of a cylinder $C_\epsilon = \{(\rho, \theta, z) \mid \rho = \epsilon (< 1)\}$ where ϵ can be arbitrarily small; the vertical arcs can be associated with leave segments in the characteristic foliation of a cylinder $C_R = \{(\rho, \theta, z) \mid \rho = R (> 1)\}$ where R can be arbitrarily large; and, a horizon-

tal arc is connected to a vertical arc by Legendrian segment that correspond to $\{(\rho, \theta_0, z_0) \mid \epsilon \leq \rho \leq R\}$ where $z = z_0$ is the plane containing the endpoint of the horizontal arc and $\theta = \theta_0$ is the half-plane containing the endpoint of the vertical arc. (So these connecting Legendrian segments are “suspensions” of the corners of the rectangular diagram.) Now smooth the corners of this piecewise Legendrian knot to obtain a smooth Legendrian knot. (Readers familiar with classical presentations of Legendrian knots should realize that what we obtain is a “braided front projection” of a Legendrian knot.) The classical invariants—the Thurston-Bennequin number tb and the rotation number r —are easily computed from the combinatorial information in such a diagram [Ma]. The Thurston-Bennequin number is the braid index less the number of upward oriented vertical arcs— $tb(K) = \text{writhe}(K) - \#(\uparrow)$. The rotation number is the writhe less the number of upward oriented vertical arcs— $r(K) = n - \#(\uparrow)$.

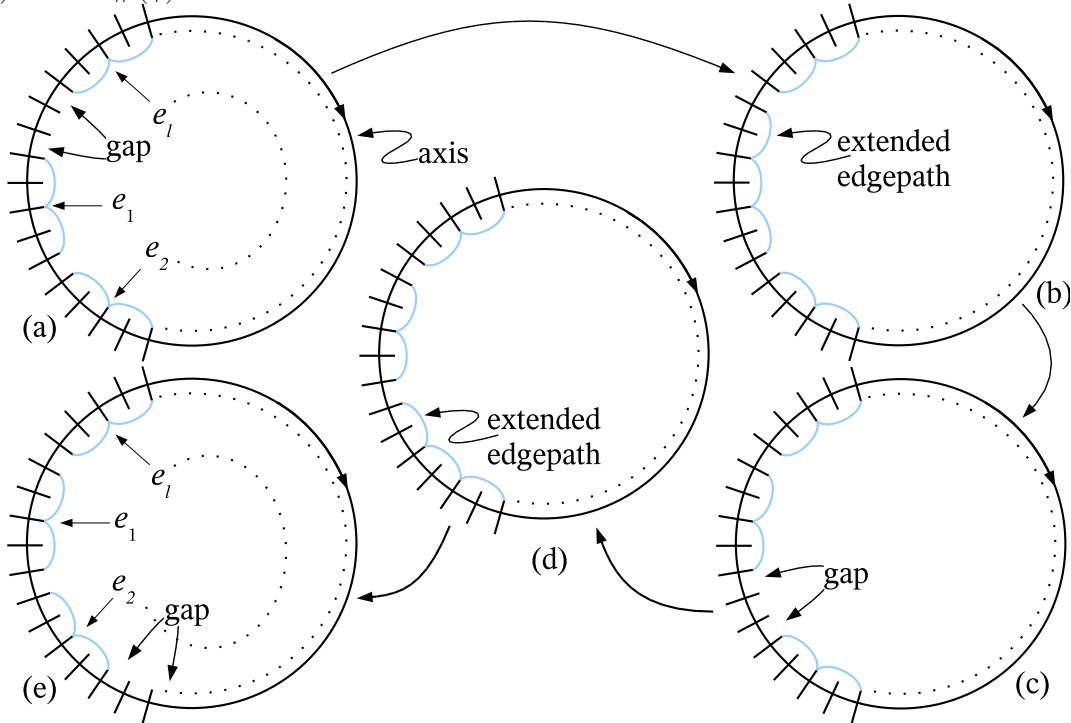


Figure 12: The extended edge-paths in (b) and (d) correspond to the λ_j -leaves mentioned in the description of interlocking in §1. Notice that the gap is consistently “rotating” in the same direction. This implies homogeneous twisting. Notice that the extended edge-path in (b) must occur before the extended edge-path in (d) can occur. This implies interlocking.

We start with our cabling coefficient $\{(p_1, q_1), (p_2, q_2), \dots, (p_{h-1}, q_{h-1})\}$ and a fixed number k coming from condition (3) of the description of rectangular block presentation. From these values we will construct an initial intersection set $\mathcal{R}_{K(P', Q')}^s \cap H_{\theta_0} \subset$

H_{θ_0} . The reader should consult Figure 12(a) as our construction advances.

There will necessarily be $[(2k + 3)(\prod_{1 \leq i \leq h-1} p_i) + 2]$ points in the set $\mathcal{R}_{(P',Q')}^s \cap \mathbf{A}$. So we realize these points of intersection in Figure 12(a) by placing down $[(2k + 3)(\prod_{1 \leq i \leq h-1} p_i) + 2]$ arcs that transversely intersect the axis \mathbf{A} . Each such arc corresponds the two radial leaves of a Δ_i -disc used in the step configuration adjoined together at their common endpoint in \mathbf{A} . In Figure 12(a) we will use the disc that \mathbf{A} visually bounds in the page as own initial H_{θ_0} . Own construction builds on the radial leaves coming from the $\Delta_i \cap H_{\theta_0}$ that are inside this visual disc. The endpoints of these radial arcs inside H_{θ_0} will necessarily be the points ϱ – points mentioned in the description of an interlocking \mathcal{R}_X .

Next, picking an initial point of $z_1 \in \Delta_1 \cap \mathbf{A} \subset \mathcal{R}_{K(P,Q)} \cap \mathbf{A} \subset \mathbf{A}$ we cyclically enumerate all there other z_j -points in this set as we transverse \mathbf{A} in the direction opposite to its orientation. (To obtain the homogeneous feature for $\mathcal{R}_{K(P',Q')}^s$ we will need to pay attention to the orientation direction of our labeling. One can obtain an alternate construction by reversing all orientations.) We place an edge-path of length k in H_{θ_0} that connects the leaves of $(\Delta_1 \cap H_{\theta_0}), (\Delta_3 \cap H_{\theta_0}), \dots, (\Delta_{\text{odd}} \cap H_{\theta_0}), \dots, (\Delta_{3+2k} \cap H_{\theta_0})$. (This edge-path corresponds to the intersection of H_{θ_0} with k consecutive R_i rectangles in the step configuration.) More generally, the pattern is to connect every-other leaf in the first $2k + 3$ leaves together by an edge-path. So starting at the leaf associated with z_{2k+4} we again connect every-other leaf by an edge-path of length k . We reiterate this edge-path connecting pattern around the radial leaves in H_{θ_0} until we have placed $(\prod_{1 \leq i \leq h-1} p_i)$ -connecting edge-paths of length k in H_{θ_0} . Thus, our every-other pattern of length k edge-paths will have accounted for $(2k + 3)(\prod_{1 \leq i \leq h-1} p_i)$ radial leaves in H_{θ_0} and each edge-path is a leaf in the foliation of k consecutive R_i rectangles in the step configuration. Our description of the initial H_{θ_0} is complete.

Figure 12 illustrates the situation when $k = 1$. The edge-paths are labeled $\{e_1, \dots, e_l\}$ where $l = (\prod_{1 \leq i \leq h-1} p_i)$. In order to obtain our homogeneous feature the direction of our labeling is again opposite the orientation of \mathbf{A} . The two-arc gap between edge-path e_1 and e_l is also indicated.

We are now in a position to describe how the H_{θ} -sequence progress so as to allow for interlocking homogeneous twisting cabling. The reader should consult the sequence of illustrations in Figure 12.

As we push H_{θ_0} forward in the fibration \mathbf{H} we will encounter the first leaf in the

foliation of $\mathcal{R}_{K(P',Q')^s}$ that intersects $k + 1$ of the R_i rectangles, i.e. where condition (vii) of the step configuration is occurs and this is necessarily a λ_j -leaf coming from the description of interlocking. This can only happen when one of the edge-paths of length k in H_{θ_0} is extended to an edge-path of length $k + 1$ (which is a λ_j -leaf) by adjoining to it one of the two-arcs associated with the gap. After passing through the fiber containing this extended Agathe immediately revert back to having all edge-paths being of length k . However, such a sequence must also yield homogeneous twisting while maintaining the interlock nature of $\mathcal{R}_{K(P',Q')^s}$.

To start this sequencing we focus on achieving the cabling associated with the first pair, (p_1, q_1) of (P', Q') . Specifically, we have the edge-path e_1 extend to a length $k + 1$ edge-path that adjoins to a radial arc associated with the gap so that the every-other radial arc pattern is maintained. (As mentioned, this extended Agathe corresponds to, say, λ_{j_1} leaf in the description for interlocking.) We then have e_1 immediately revert back to an edge-path of length k . We can do this sequence in such a fashion that the gap is “rotated” past e_1 .

Referring to the change from Figure 12(a) to 12(b) to 12(c) we see that e_1 's length goes from 2 to 3 back to 2. Notice that the gap has been moved so as to be between e_1 and e_2 where its initial position was between e_1 and e_l . This sequence constitutes a partial positive twisting. Continuing we can move the gap past all edge-paths e_2 through e_l . In doing so we pass through edge-paths λ_{j_2} through λ_{j_l} . We can then reiterate this gap moving sequence so as to achieve twisting corresponding to (p_1, q_1) . (We are not addressing the question of which (p_1, q_1) is realizable—the answer to this question will involve an interplay between (P, Q) and k .)

By always rotating the two-arc gap in the same direction it is easy to check that we have homogeneous twisting. Simply designate a point on \mathbf{A} as $\{\infty\}$ and verify that the triple inequality for any triple $(z_{i-1}^4, z_i^4, z_{i+1}^4)$ is satisfied. Seeing that we also have interlocking is also straight forward. Just notice that the edge-path λ_{j_1} must disappear before the edge-path λ_{j_2} can occur as we advance through the H_θ -sequence.

Now we achieve the cabling associated with the second pair, (p_2, q_2) of (P, Q) . For the purpose of simplifying our indexing notation, after finishing the cabling/twisting associate with (p_1, q_1) , we relabel our edge-paths so that again the two-arc gap is between e_1 and e_l . Again we require that our direction of labeling be opposite the orientation of \mathbf{A} . We now draw an imaginary proper arc across H_{θ_0} that is away from our radial arcs and edge-paths which splits off the edge-paths e_1 through $e_{(p_2 \times \dots \times p_{h-1})}$

along with the two-arc gap. Call this split off sub-fiber disc $H_{\theta_0}^2 \subset H_{\theta_0}$. Notice that this sub-fiber is configured similar to our initial H_{θ_0} except with $\prod_{2 \leq i \leq l} p_i$ edge-paths (along with the two-arc gap). We can then repeat our twisting H_{θ} -sequence only restricted to $H_{\theta_0}^2$. (Again, we are not addressing the question of which (p_2, q_2) is realizable.)

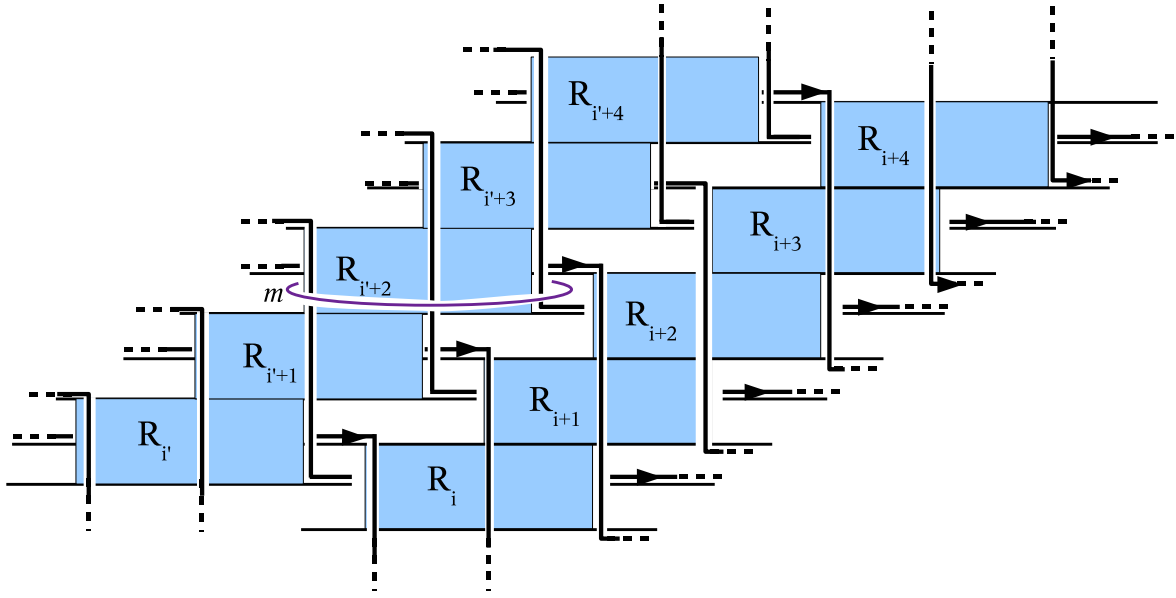


Figure 13: We require that within a neighborhood of every λ_j -leaf there be a vertical arc of the rectangular diagram of $K_{(P,Q)}$; and, within a neighborhood of every segment of $\partial\Delta_i$ where an R_i -rectangle is not attached there be a horizontal arc of the rectangular diagram. The meridian curve m will necessarily link $K_{(P,Q)}$ at least $k + 1$ times. Thus, $p_h \geq k + 2$.

In general, through a sequence of sub-fiber discs—splitting off $p_3 \times \dots \times p_l$ edge-paths, then $p_4 \times \dots \times p_l$ edge-paths and so on—we can iterate the underlining cabling/twisting of Figure 12 to obtain the H_{θ} -sequence for $\mathcal{R}_{K(P,Q)}^s$. Always relabeling the edge-paths in the opposite direction of \mathbf{A} 's orientation will yield our homogeneous twisting feature. Again, this can be directly verified by checking the triple inequality condition for a z_i -triple. (Reversing all orientations will yield an alternative construction.) The every-other pattern of our edge-paths will yield our interlocking feature because, again, the extended edge-paths correspond to our λ_j -leaves. Although care is required, a geometric realization of $\mathcal{R}_{K(P,Q)}^s$ coming from such an H_{θ} -sequence can readily be produce. A useful format for visualizing such a realization, as we shall shown in §6, is a square diagram that identifies the left & right sides and the top & bottom sides. (Jump ahead and see Figure 14.)

We now appeal to Figure 13 to illustrate how the knot $K_{(P,Q)}$ can be superimposed over the a geometric realization of $\mathcal{R}_{K(P',Q')}^s$. Specifically, $K_{(P,Q)}$ will be represented utilizing a rectangular diagram where the horizontal arcs will be line segments that are parallel and in neighborhoods of the $\partial\Delta_i \subset \mathcal{R}_{K(P',Q')}^s$ and the vertical arcs are in neighborhoods of the edge-path/leaves that are of length $k + 1$. For the interlocking feature to be obtain we require that there be at least vertical arc associated with every such $k + 1$ length λ_j -edge-path and every segment of $\partial\Delta_i$ not having an R_i rectangle attached have an associate horizontal arc. In Figure 13 also illustrates that $p_h \geq k + 2$

In the next section we work out an explicit example.

6 Appendix: The $(2, 3)$ cabling of the $(2, 3)$ torus knot. (Joint with H. Matsuda.)

With the general construction of $\mathcal{R}_{K(P,Q)}^s$ in mind along with the corresponding rectangular diagram representation of $K(P, Q)$ we will now discuss the explicit representations to the $(2, 3)$ cabling of the $(2, 3)$ torus knot (the positive trefoil) that was implicitly discovered in Theorem 1.7 of [EH]. Specifically, their theorem says that there exists two transversal knots those knot type is $K_{((2,3),(2,3))}$ having Bennequin number equal to 3 but are not transversal isotopic. The examples in this section are collaborative with H. Matsuda.

From Theorem 1 we know that likely candidates for explicit presentations could come from rectangular block presentations of the positive trefoil that have homogeneous twisting and are interlocking. Such a presentation was first discovered in [P] and is illustrated in Figure 14. A brief pictorial narrative is useful. Figure 14 can best be thought of initially as the projection of $\mathcal{R}_{K(2,3)}^s$ onto the unit cylinder \mathcal{T}_1 which is then made into a torus by identifying the two ends at infinity. Thus, the two “half-blocks” at the top are identified with the two “half-blocks” at the bottom. Once this understanding is focused in one’s mind the radial discs $\{\Delta_1, \dots, \Delta_{11}\}$ are added to form the steps configuration. The labels for these radial disc are the right side column of numbers. In addition we indicate two meridian curve, m & m' that would correspond in type to the $m_{i+.5}$ meridian curves in Figure 6, i.e. in the foliation of \mathcal{T}_C they pass through a negative and positive singularity. Any $(2, 3)$ cabling will then have to link these two meridians three times.

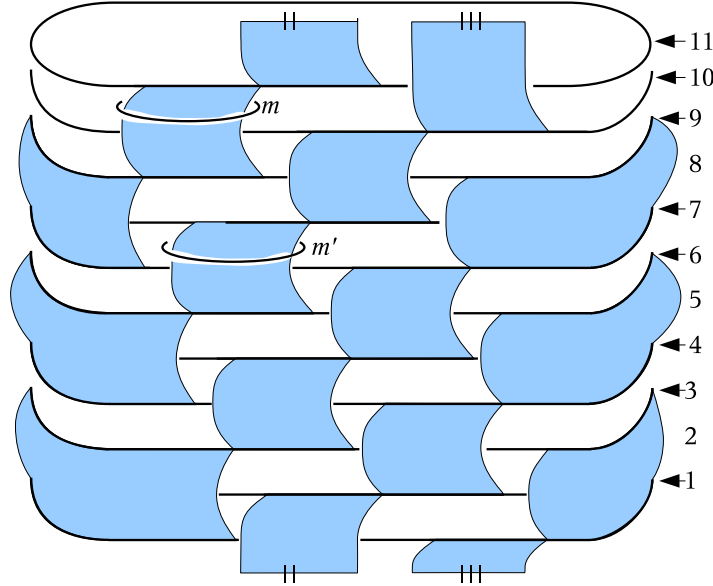


Figure 14: The steps configure illustrated here has three of its rectangle discs wrap around behind the illustration and two of its rectangle discs go up “through infinity” and return from below. (Or equivalently, the left and right sides are identified; and the top and bottom are identified.)

Finally, referring back to conditions (3) of our definition of rectangular block presentations and (vii) of our step configuration, we note the $k = 0$ for Figure 14. Thus, each λ -leaf in $\mathcal{R}_{K_{((2,3),(2,3))}}^s$ is just $r_i^3 \cup r_{i+1}^1$.

Next, Figure 15 illustrates the $(2, 3)$ cabling of the torus that is the boundary of a regular boundary of the step configuration in Figure 14. Our cabling $K_{((2,3),(2,3))}$ is drawn as the rectangular diagram projection onto \mathcal{T}_1 with ends identified again. The columns of numbers that are to the right of the projection are meant to correspond to the radial disc labels in Figure 14. Therefore, although it makes for a very busy illustration one could superimpose Figure 15 onto Figure 14 to understand how $K_{((2,3),(2,3))}$ is positioned in a neighborhood of $\mathcal{R}_{K_{((2,3),(2,3))}}^s$ and, thus, $\mathcal{T}_C \mathcal{T}_C$. Amongst this ambitious visualization we have depicted the corresponding meridian curves m & m' in Figure 15 that each link $K_{((2,3),(2,3))}$ three times.

We can now consider the two alternate interpretations of our rectangular diagram in the standard contact structure.

From the Legendrian perspective we see that Figure 15 depicts a Legendrian knot corresponding to one describe in Theorem 1.9 of [EH]. Its Thurston-Bennequin number is 5 and its rotation number is 2. (See Figure 1 of [EH].)

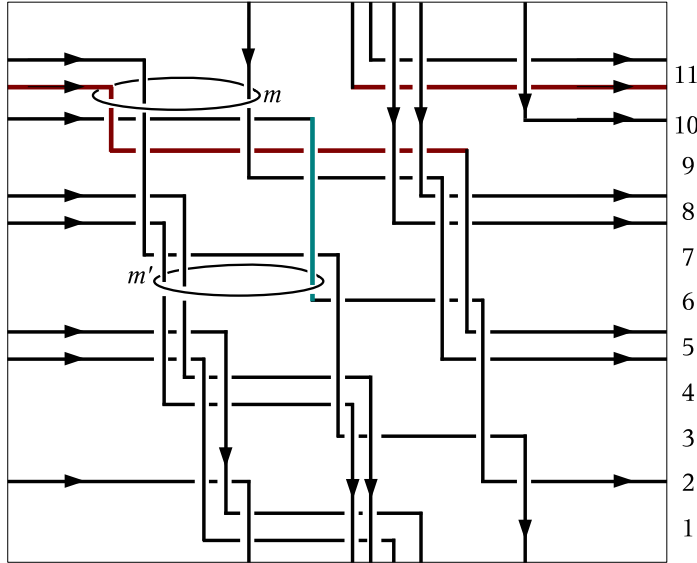


Figure 15: The illustration should be seen as a rectangular diagram projected onto a torus. The top side of the diagram is identified with the bottom side; and the left side is identified with the right side.

If we take the associated transversal braid from Figure 15 the Bennequin number for $K_{((2,3),(2,3))}$ is readily computed: the braid index is 8 and the algebraic length is 11. Then $K_{((2,3),(2,3))}$ has a transversal knot presentation with Bennequin number 3.

Finally, in Figure 15 we have colored two portions of the diagram. The portion is a single vertical turquoise arc and the other is a red edge-path. The red edge-path has angular length in the braid a little greater than 2π . Together these two portions indicate the existence of a negative elementary flype. A useful source for thinking about negative elementary flypes is [BM1] and, in the situation for transversal knots, [BM2]. Specifically, in [BM2] it was established that transversal knots that are presented as closed 3-braids and are related to each other via negative elementary flypes have the same Bennequin number but are not transversally isotopic in the standard contact structure. Our goal is to illustrate that the two differing transversal classes of $TK_{((2,3),(2,3))}$ are also related by a negative flype.

This goal is achieved by simply depicting the rectangular diagram resulting from applying the indicated negative elementary flype. (See Figure 1(c).) Figure 16 illustrates the resulting diagram. The turquoise edge-path corresponds to a negative stabilization of the vertical turquoise arc in Figure 15; and the red vertical arc corresponds to a negative destabilization of the red edge-path in Figure 15. The meridian

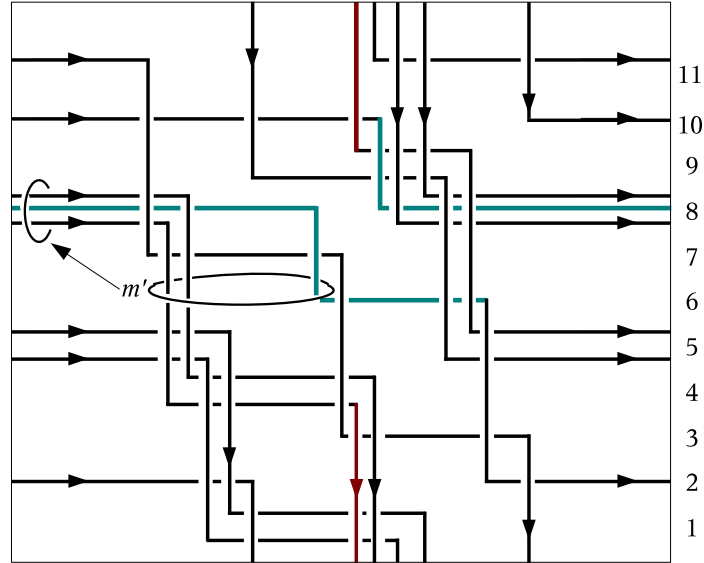


Figure 16: As in Figure 15 the illustration should be seen as a rectangular diagram projected onto a torus.

curve m' has been undisturbed by the flype but it can now be isotoped so that it is vertical, i.e. there is some $H_\theta \in \mathbf{H}$ such that $m' \subset H_\theta$. This implies that the resulting cabling torus has a circular leaf and must then have a mixed foliation. But once we have the cabling torus possessing a mixed foliation, by Proposition 4.1[M1] through a sequence of braid isotopies, exchange moves and destabilizations we can produce a foliation with only \mathbf{c} -circles. Thus, after the negative flype we can reduce our cabling down to the obvious braid representation.

To connect the dots in our discussion, when viewed as closed transverse braids in the standard contact structure, the pair of braids in Figures 15 and 16 must correspond to the implicit pair in Theorem 1.7 of [EH]. In particular, by Theorem 1 we know that if there is more than the transversal class that corresponds to the exchange reducible class then such a class when viewed as a classical braid will yield an interlocking homogeneous twisting rectangular block presentation for which it is a cabling. Since Figure 14 illustrates such a presentation and since by Theorem 1.7 [EH] there are exactly two transverse isotopy classes in $TK_{((2,3),(2,3))}$ having Thurston-Bennequin invariant 3. We know Figure 16 must be one (the exchange reducible class) and Figure 15 must be the other.

Finally, if we decide to view the rectangular diagram as representing a Legendrian diagram one can readily check that its classical invariants have not be altered (again,

see [Ma]). So the Legendrian “diagrams” of Figures 15 and 16 represent one of the points of multiplicities in Figure 1 of [EH], i.e. two differing Legendrian classes that have the same knot type and classical invariants $tb = 5$ and $r = 2$ as corresponding to the multiplicity 2 entry in Figure 1 of [EH].

Three concluding remarks are in order. First, it is interesting to note that negative elementary flypes (Figure 1(c)) are to date the only method for producing explicit examples of transverse knots that are of the same knot type having the same classical invariant, but are not transversally isotopic. (In [BM2] it was established that 3-braids related by negative elementary flypes produced such examples.) Second, the question arises whether the MTWS braid calculus [BM1] for cable knots is only destabilizations, exchange moves and elementary flypes (or, maybe weighted elementary flypes). Third, understanding the connection between an interlocking homogeneous twisting standard cabling torus and the Etnyre-Honda uniform thickness property is a natural direction for future research. The reader should realize that construction of $\mathcal{R}_{K(P,Q)}$ in §5 can be varied by altering the sequencing choice of the sub-fiber discs and the cabling/twisting illustrated in Figure 12. This spectrum of choices is conceivable a source of further examples of transversal/Legendrian knots having the same classical invariants but multiple transversal/Legendrian classes.

References

- [B] D. Bennequin, *Entrelacements et équations de Pfaff*, Astérisque **107-108** (1983). 87-161.
- [BF] J. Birman and E. Finkelstein, *Studying surfaces via closed braids*, Journal of Knot Theory and Its Ramifications, Vol. 7, No. 3 (1998), 267-334.
- [BM1] J. Birman and W. Menasco, *Stabilization in the braid groups-I: MTWS*, Geometry & Topology 10 (2006), 413-540.
- [BM2] J. Birman and W. Menasco, *Stabilization in the braid groups-II: Transversal simplicity of knots*, Geometry & Topology, 10 (2006) 1425-1452.
- [BW] J. S. Birman and N. C. Wrinkle, *On transversally simple knots*, J. Differential Geom. 55, no. 2 (2000), 325-354.

- [C] P. Cromwell, *Embedding knots and links in an open book I: Basic properties*, Topology and Its Applications 64 (1995), 37-58.
- [D] I.A. Dynnikov, *Arc-presentations of links. Monotonic simplification*, Fund. Math. 190 (2006), 29–76.
- [EH] J. Etnyre and K. Honda, *Cabling and transverse simplicity*, Ann. of Math. (2) 162 (2005), no. 3, 1305–1333.
- [Ma] H. Matsuda, *Links in an open book decomposition and in the standard contact structure*, preprint, 2004.
- [M1] W. Menasco, *On iterated torus knots and transversal knots*, Geometry & Topology, Vol. 5 (2001) Paper no. 21, 651–682.
- [M2] W. Menasco, *Erratum: On iterated torus knots and transversal knots*, Geometry & Topology 5 (2001), 651–682, eprint at arXiv, math.GT/0610565
- [N] K.Y. Ng, *Essential tori in link complements*, J. of Knot Theory and Its Ramifications, **7**(1998), 205–216.
- [P] V. Pinciu, *Positioning of Essential Surfaces in Link Complements*, PhD thesis, University at Buffalo, 1998.